Journal of Applied Mechanics and Technical Physics, Vol. 37, No. 6, 1996

AN EXPERIMENTAL STUDY OF DENSITY FLUCTUATIONS IN THE HYPERSONIC BOUNDARY LAYER ON A FLAT PLATE

A. A. Maslov, S. G. Mironov, and A. N. Shiplyuk

UDC 532.526

The stability of hypersonic flows is a very important problem in designing heat-protection systems for recoverable spacecraft and hypersonic aircraft. A great number of theoretical and experimental investigations of the stability of sub- and supersonic flows have been carried out. However, the results of these studies cannot be completely applied for high hypersonic Mach numbers because of the qualitative features of flow and the development of disturbances under these conditions [1]. On the other hand, the experimental studies of disturbance characteristics for free-stream Mach numbers $M_\infty > 8$ [2–7] are few in number. In these studies, only some disturbance characteristics have been obtained, and they are hardly comparable because of the considerable differences in conditions of measurements. This is due to the difficulty of constructing special hypersonic facilities and with the problems of using traditional aerodynamic methods of disturbance measurements in low-density flows with a high stagnation temperature, which are typical of hypersonic wind tunnels.

The electron-beam technique [8, 9] has obvious advantages under these conditions. It allows the density to be measured in rarefied flows. Fluctuations in the boundary layer on the walls of the working section of a wind tunnel [2, 3] and in the shear layer in the Eiffel chamber of a hypersonic wind tunnel [4] have been studied using this method.

In most continuous-hypersonic wind tunnels, it is not possible to ensure the high Reynolds numbers necessary for transition studies. Nevertheless, it is important to study the characteristics of initial disturbances near the leading edge of a body at which a laminar flow occurs. These disturbances affect substantially the development and spectrum of disturbances preceding the laminar-turbulent transition. For low unit Reynolds numbers, a detailed spatial study of the characteristics of these initial disturbances is possible in a comparatively thick hypersonic boundary layer.

A method of density and density-fluctuation measurements in hypersonic flows using electron-beam fluorescence of nitrogen is described in the present paper. The method allows one to obtain spectra, phase velocities, spatial correlations, wave-propagation angles, and growth rates of natural disturbances. The characteristics of density fluctuations in a hypersonic boundary layer on a flat plate with a sharp leading edge at zero angle of attack were studied for $M_\infty = 21$ and $T_w/T_0 = 0.26$–0.29 (T_w is the model surface temperature and T_0 is the stagnation temperature) for Reynolds numbers $Re_x = 2.6 \cdot 10^4$–$1.7 \cdot 10^5$ calculated from the longitudinal x coordinate and free-stream parameters.

1. Experimental Equipment. The measurements were performed in a T-327 hypersonic nitrogen wind tunnel at the Institute of Theoretical and Applied Mechanics, Siberian Division, Russian Academy of Sciences [10]. The tunnel includes a graphite gas heater in the nozzle plenum chamber, a device for shock starting, and a system of gas exhaust into a vacuum chamber. The running time is 30 sec. Stagnation pressure and temperature were kept constant during the measurements ($P_0 = 8$ MPa and $T_0 = 1100$ K). Under these conditions, the following parameters are obtained in the working section: $M_\infty = 21$, absolute velocity value $U = 1500$ m/sec, unit Reynolds number $Re_1 = 6 \cdot 10^5$ m^{-1}, and gas density $n_\infty = 7 \cdot 10^{21}$ m^{-3}. The radius of the uniform flow core is $5 \cdot 10^{-2}$ m. The density drops down outside the core, reaching $\cong 6 \cdot 10^{20}$ m^{-3} at a distance of 0.1 m from the axis.

Institute of Theoretical and Applied Mechanics, Siberian Division, Russian Academy of Sciences, Novosibirsk 630090. Translated from Prikladnaya Mekhanika i Tekhnicheskaya Fizika, Vol. 37, No. 6, pp. 51–60, November–December, 1996. Original article submitted August 14, 1995.

 0021-8944/96/3706-0816 $15.00

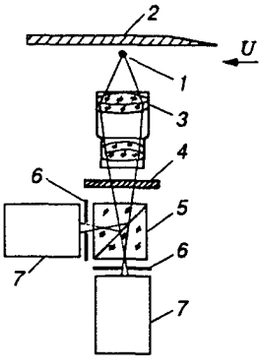

Fig. 1

The plate model had a tapered shape. The leading-edge width was $8 \cdot 10^{-2}$ m, the trailing-edge width was $6 \cdot 10^{-2}$, the plate length was $L = 0.36$ m, and its thickness was $5 \cdot 10^{-3}$ m. The nose cone angle was 7° and the leading-edge radius was less than $5 \cdot 10^{-5}$ m, which is comparable with the free path of free-stream molecules. The plate was made of blackened aluminum. In the course of the experiment, the plate temperature T_w was varied within the range 290–320 K.

The gas-flow density was determined from the intensity of nitrogen fluorescence under the action of the probing electron beam. The electron energy was 12 keV, the beam current was not higher than 1 mA, and its diameter under high vacuum conditions was 10^{-3} m. A diagram of the optical measurements is shown in Fig. 1. The electron beam 1 propagated across the flow parallel to the plane of plate 2. Scanning of the flow-field on the plate was performed either by cross-flow displacement of the plate from $-2 \cdot 10^{-2}$ to $+3 \cdot 10^{-2}$ m relative to the flow axis, or by deflecting the electron beam by a magnetic system. Flow-field scanning along the plate was performed by combining beam deflection and electron-gun displacement.

The optical system for nitrogen-fluorescence recording included a wide-angle lens 3, an SS-8 glass filter 4 with a transmission band of 360–500 nm, a light-splitting cube 5, and diaphragms 6, which confined the field of vision of FEU-79 electron photomultipliers (EPM) 7 within $1.7 \cdot 10^{-3}$ m across the beam and 10^{-2} m along it. The direction of the observation axis coincided with the normal to the plate surface. A measurement of the composition of the light entering the EPM using an SPM-2 spectrometer showed that the spectrum corresponds to the emission of the first negative and second positive bands with a ratio of the total intensities of 7 : 1.

The values of the average and fluctuating components of the output signals of the EPM were increased by U7-5 and RU11-12 amplifiers and recorded separately by an N067 multichannel magnitograph. The noise at frequencies up to 500 Hz was eliminated from the signal. The signal was recorded on the magnitograph in the frequency-modulation regime in the range of up to 40 kHz. The other magnitograph channels recorded simultaneously the signals of displacement sensors and the electron current on the collector.

The optical range and simplified scheme of spectral filtration of radiation was used because of the necessity of obtaining an intense light flux for measurements over a wide frequency range of density fluctuations without using the procedure of signal accumulation. This made it possible to study natural disturbances in the flow. In spite of the measures taken, the light flux from the observation region is not sufficiently intense, and the signal determined by the density fluctuations is obscured by the intense wide-band "shot" noise related to the discrete nature of photocurrent. To exclude this noise, we used the "cross-correlation" method, in which a cross-spectral signal of two EPM recording the emission from the same fluorescence region is found. As a result, the cross-spectrum contains the portion of the signal that is common for the two EPM and caused only by the density fluctuations at the observation point.

The optical system (Fig. 1) allows for both one-point measurements of density and density fluctuations, in which the emission from the same region enters both EPM, and two-point measurements, in which fluorescence from two observation points is recorded. The electron beam is split into two parts by supplying

the "meander-type" voltage to the magnetic system. The field of vision of each EPM is adjusted to the position of thus-formed two electron beams by rotation of the light-splitting cube. The frequency of beam oscillations was 20 kHz. The distance between the measurement points was varied by the sweep voltage up to $1.7 \cdot 10^{-2}$ m.

The magnitograph records were processed using the CAMAC system on an IBM-486.

2. Technique for Measuring Density and Density Fluctuations. A direct quantitative density determination using electron-beam fluorescence is possible only if there is a linear relationship between the light intensity and gas density. In this case, to find absolute values of density, one should know only the slope of the calibration curve, which depends on the beam current and the effectiveness of emission collection by the optical system. If the calibration curve is not linear, the light intensity at the observation point is determined not only by the local gas density but also by the density upstream of the electron beam. The possible causes of the nonlinearity are discussed in [9]. An analysis of the calibration curves obtained in [4, 8, 11, 12] for comparatively high nitrogen pressures leads to the conclusion that beam electron scattering has a dominant influence on nonlinearity of the curves for densities lower than $\approx 2 \cdot 10^{22}$ m^{-3}.

The linearity broken, the problem of finding the density at a point from the fluorescence intensity cannot be solved in the general case. However, quantitative density data can be obtained in the following special cases.

(A) The problem can be solved for two-dimensional gas objects that are uniform along the electron beam and nonuniform in the transverse direction. Examples of such objects are flows on a flat plate, wedge, etc. that are oriented parallel to the probing beam. The spanwise dimensions of the model in flow should be similar or larger than the free-stream flow dimension (flow core). In this case, the density can be found from the calibration curve $I = \Psi(n)$ obtained for free hypersonic flow in the wind tunnel (I is the output signal of the optical system of fluorescence registration). The observed difference in static temperature does not have a noticeable effect on density measurements within our range of stagnation temperatures and gas densities [12]. Since the calibration curve depends on the observation point, for uniqueness, one can choose the point on the flow axis using the flow two-dimensionality. To eliminate the influence of the beam current on the calibration curve, the curve is represented in dimensionless form: $I/I_\infty = \Psi(n/n_\infty)$. The relation $\Psi(n/n_\infty)$ can be conveniently represented as the product of the linear and nonlinear terms, $\Psi(n/n_\infty) = A\,(n/n_\infty)\,\xi\,(n/n_\infty)$, where A is a coefficient the determines the slope of the linear section and the function $0 < \xi(n/n_\infty) \leqslant 1$ describes the decrease in the beam current density due to scattering in the gas.

If there are two-dimensional density fluctuations (two-dimensional waves) in the flow, their characteristics can be measured. The variable component of the output signal I'/I_∞ is related to the fluctuations n'/n_∞ by

$$\frac{n'}{n_\infty} = \frac{I'}{I_\infty} \Big/ \frac{\partial \Psi}{\partial n} \qquad (n' \ll n). \tag{2.1}$$

It follows from (2.1) that the density fluctuations depend not only on the variable signal component but also on the mean density as $\partial\Psi/\partial n$.

(B) The problem can be solved for three-dimensional gas inhomogeneities which are located in a flow with uniform density and disturb weakly the probing beam. Let us define the condition for weak disturbances of the probing beam. The current density of electrons $j(z)$ coming to the observation point z (z is the transverse coordinate) is described by

$$j(z) = j_0 \exp\Big\{ -\sigma \int_0^z (n + n')dr \Big\}, \tag{2.2}$$

where j_0 is the initial beam current density, σ is the cross section of the elastic and inelastic electron scattering by molecules, n is the mean free-stream density, and n' is the density fluctuation on the scale l of the gas inhomogeneity. Expression (2.2) can be transformed to the form

$$j(z) = j_m \exp\Big\{ -\sigma \int_0^z n' dr \Big\}. \tag{2.3}$$

Here $j_m(z) = j_0(z)\exp\left\{-\sigma\int_0^z ndr\right\}$ and $j_m(z)$ is the beam current density at point z outside of the inhomogeneity. If the disturbance is weak, we have $j(z) \cong j_m(z)$, which corresponds to the condition

$$\sigma\int_0^z n'dr \ll 1 \tag{2.4}$$

or

$$\sigma\int_0^l n'dr \ll 1. \tag{2.5}$$

Taking into account that $I(z) \approx j(z)n(z)$, from (2.3) and (2.5) we have $I' \approx j_m(z)n'$. This means that no marked additional scattering of the beam occurs over the inhomogeneity length l and there is a linear relationship between the deviation of local density from the mean value and the deviation of light intensity from its value in the undisturbed flow. This allows one to obtain quantitative data on the relative density values in such inhomogeneities.

We now define conditions for measuring the characteristics of density fluctuations such as three-dimensional waves in a two-dimensional flow. Since the output signal of the optical system is proportional to the product of gas density and beam current density, its variable component in a first approximation takes the form

$$I' \approx nj' + jn', \tag{2.6}$$

where j and j' are the mean values of current density and current density fluctuations at the observation point. The presence of current density fluctuations is caused by the probing beam electron scattering by the density fluctuations of the wave packet propagating upstream of the electron flow. It follows from (2.3) and (2.4) that

$$j'(z) = j(z)\exp\left\{-\sigma\int_0^z n'dr\right\}. \tag{2.7}$$

Let us represent n' by a wave traveling across a two-dimensional flow:

$$n' \approx \exp(i\beta z)\exp(-i\omega t)\exp(i\varphi). \tag{2.8}$$

Here $\beta = 2\pi/\lambda_z$ is the spanwise wavenumber, ω is the rotational frequency, and φ is the phase. We consider three possible cases.

In the first case,

$$l_c \cong z, \qquad \lambda_z \ll z, \tag{2.9}$$

where l_c is the characteristic length of random variations in the wave phase (the coherence length). The integral in (2.7) is close to zero because of the rapid oscillations of the first factor in (2.8), and the term containing j' in (2.6) can be ignored.

In the second case,

$$l_c \cong z, \qquad \lambda_z \cong z. \tag{2.10}$$

In this case, all terms in (2.6) must be taken into account, and the density-fluctuation measurements are no longer spatially local.

In the third case,

$$l_c \ll z, \qquad \lambda_z > l_c. \tag{2.11}$$

The integral in (2.7) is close to zero due to the random oscillations of the third term in (2.8) over a length greater than l_c, and the terms with j' in (2.6) can also be ignored.

If conditions (2.5), (2.9), or (2.11) are satisfied, local measurements of three-dimensional density fluctuations can be performed in two-dimensional flows by the electron-beam method. Within the framework of this approach, we write the conditions of measurement of purely two-dimensional density fluctuations as follows: l_c is an arbitrary number and $\lambda_z \gg z$.

Let us determine the relationship between three-dimensional density fluctuations and the variable component of the output signal. From (2.3) and (2.5), we have $I' = kjn'$ and $I_\infty = kj_\infty n_\infty$, where k is a proportionality coefficient that takes into account the aperture ratio of the optical system, the effectiveness of gas excitation by electrons, the geometry of the observation region, etc. It follows herefrom that $I'/I_\infty = (j/j_\infty)(n'/n_\infty) = (jj_0/j_0j_\infty)(n'/n_\infty)$. If the electron scattering process in the gas is dominating, we obtain $j/j_0 \approx \xi(n/n_\infty)$ and $j_\infty/j_0 \approx \xi(n_\infty/n_\infty) = \xi(1)$, and, hence,

$$\frac{n'}{n_\infty} = \frac{\xi(1)}{\xi(n/n_\infty)} \frac{I'}{I_\infty}.$$

In one-point measurements, the spanwise distributions of the integral and spectral characteristics of density fluctuations are determined [dimensionless levels of fluctuations n'/n_∞ and fluctuation spectra $n'(\omega)/n_\infty$]. The spectral quantities are found by creating arrays of Fourier coefficients by means of a fast Fourier transform and formation of spectral functions using the following relations [13]:
the cross-spectrum

$$I_{12}(\omega) = \sqrt{Q_{12}^2(\omega) + R_{12}^2(\omega)} = I', \quad Q_{12}^2(\omega) = A_1A_2 + B_1B_2, \quad R_{12}^2(\omega) = A_1B_2 - B_1A_2,$$

and the phase spectrum

$$\varphi_{12} = \arctan(Q_{12}/R_{12}).$$

Here A_1 and A_2 are Fourier coefficients for real terms of expansion, and B_1 and B_2 are Fourier coefficients for imaginary terms of expansion. For one-point measurements, the quantity φ_{12} has the meaning of an instrumental phase shift. The technique of two-point measurements of density fluctuations allows one to measure the phase velocity of disturbance propagation and, in addition, to obtain the coherence length of density fluctuations l_c.

Let us find the relationship between the phase shift of photomultiplier signals and phase velocity. Since the probing beam appears alternatively in the field of vision of either EPM, the phase difference $\Delta\varphi$ of two harmonic waves with rotational frequency ω has the form $\Delta\varphi = \gamma(x+\Delta x) - \omega(t+\Delta t) - \gamma x + \omega t = \gamma\Delta x - \omega\Delta t$, where $\gamma = 2\pi/\lambda_x$ is the wave vector, Δt is the time equal to the half-period of the beam oscillation, and Δx is the shift in positions of the observation points of the photomultipliers. It follows from the definition of phase velocity $c_x(\omega)$ and the expression for $\Delta\varphi$ that $c_x(\omega) = \omega/\gamma = \omega\Delta x/(\omega\Delta t + \Delta\varphi)$. Here $\Delta\varphi$ is found as the difference between the values of phase spectra obtained for $\Delta x = 0$ and $\Delta x \neq 0$.

When the fluctuations are measured, higher harmonics can be generated in the output-signal spectra. This is caused by both the nonlinearity of the function $\Psi(n/n_\infty)$ and the oscillations of the inhomogeneous density profile in the measurement region. For fairly small values of density fluctuations, the nonlinearity of $\Psi(n/n_\infty)$ can be ignored. The existence of sudden density changes in the shock-wave region with oscillations is the main source of generation of harmonics. This can be readily verified. The intensity of radiation from the region of a finite-size probing beam is described by the relation

$$I \approx \int_{-\infty}^{\infty} j(y)n(y)dy, \tag{2.12}$$

where $j(y)$ is the current distribution in the beam and $n(y)$ is the density profile (y is the normal coordinate to the plate surface). When a harmonic wave is propagating in a shock layer, the density profile is oscillating with respect to the y coordinate:

$$y' = y + a\sin(\omega t), \qquad a \ll y.$$

Expanding expression (2.12) into a series in the small parameter $a\sin(\omega t)$, we obtain the following equation

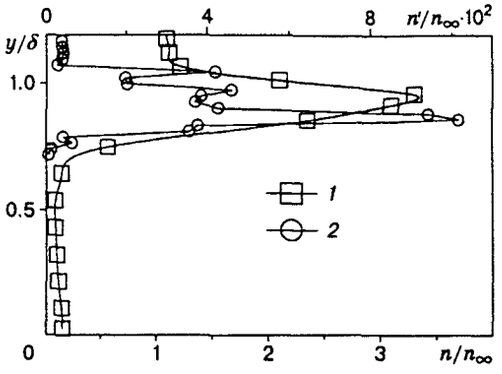

Fig. 2

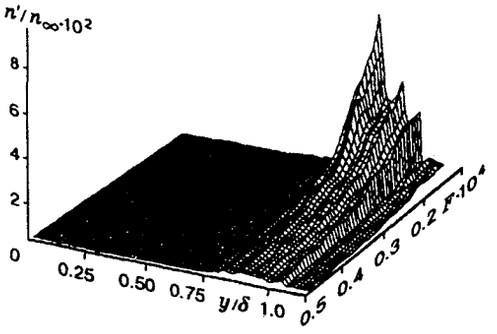

Fig. 3

for the fluctuating component of the signal:

$$I' \approx \Big[\int_{-\infty}^{\infty} j(y)\frac{\partial n(y)}{\partial y}\,dy\Big]a\sin(\omega t) + \frac{1}{2}\Big[\int_{-\infty}^{\infty} j(y)\frac{\partial^2 n(y)}{\partial^2 y}\,dy\Big]a^2\sin^2(\omega t) + \ldots$$

or

$$I' \approx a\sin(\omega t)\Big[\int_{-\infty}^{\infty} j(y)\frac{\partial n(y)}{\partial y}\,dy\Big] + \frac{a^2}{4}\cos\Big(2\omega t + \frac{\pi}{2}\Big)\Big[\int_{-\infty}^{\infty} j(y)\frac{\partial^2 n(y)}{\partial^2 y}\,dy\Big] + \ldots .$$

One can see that in the regions in which the first derivative $\partial n/\partial y$ vanishes (at the maximum of the density distribution and in the region in which the density distribution reaches a constant value in the external flow), the second- and higher-order derivatives are different from zero and give rise to harmonics. Their intensity depends on the width and shape of the electron beam and on the functional dependence of the density distribution.

The calibration dependence $I/I_\infty = \Psi(n/n_\infty)$ was obtained experimentally by recording the fluorescence intensity with variation in density at the observation point of the optical system. The density in motionless nitrogen was changed by gas inflow into the working section and was measured by a vacuum gage. In a hypersonic flow, the density at the observation point was varied by changing the stagnation pressure and was calculated by isentropic relations. The measurement results are generalized by the relation

$$\Psi(n/n_\infty) = A\,(n/n_\infty)\,\xi(n/n_\infty) = 2A\,(n/n_\infty)\Phi(b/\sqrt{n/n_\infty}) \qquad (A = 2.65; b = 0.5) \qquad (2.13)$$

within an accuracy of 6%. This relation was obtained according to the model of [14] for electron scattering in nitrogen with the Poisson distribution of the probing-beam current. Here b is the nonlinearity parameter and Φ is the probability integral. Relation (2.13) was used in this paper as a calibration curve for determining the density and density-fluctuation profiles in the two-dimensional flow over a plate. The mean density was calculated by solving Eq. (2.13) by an iterative method for each observation point.

3. Measurement Results. Figure 2 shows the normalized distributions of the mean density and the total density fluctuations (points 1 and 2) over the shock-layer height y/δ in the cross section $x/L = 0.81$ (δ is the shock-layer thickness). The fluctuations are integrated within the range of 2–16 kHz. Figure 3 shows the fluctuation distribution over the shock-layer thickness for the same cross section versus the dimensionless frequency $F = 2\pi f/(\mathrm{Re}_{1e}U_e)$ (the frequency resolution is 300 Hz). The subscript e indicates that the parameter corresponds to the value at the shock-layer edge. One can see from Figs. 2 and 3 that the major portion of fluctuations is concentrated in a narrow layer under the density drop and the fluctuation intensity decreases rapidly toward the plate surface. On the other hand, some portion of fluctuations lies in the low-frequency region of the spectrum, and the fluctuation intensity decreases considerably with an increase in the frequency.

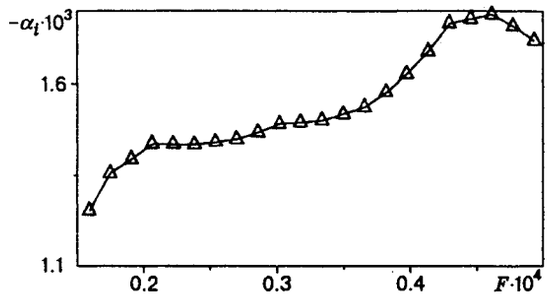

Fig. 4

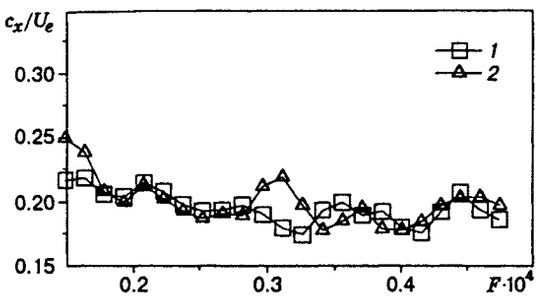

Fig. 5

The qualitative picture of amplitude–frequency distributions of density fluctuations over the shock-layer thickness is preserved over the entire range of distances from the plate tip ($x/L = 0.12$–0.81). There are two extra peaks in the distribution, which are well seen in the graph. The position of one of these peaks coincides with the maximum of the density distribution, and the other peak coincides with the external slope of the distribution.

The appearance of these peaks can be explained by fluctuations of the shock position and by the associated density distribution under the action of disturbances in the incoming flow. On the slopes of the density distribution with maximum gradients, wide-band fluctuations of light intensity arise because of density variations in the probing beam. At the same time, harmonics that also show a wide-band spectrum are generated at the maximum of density distribution and at the external edge of the shock. The high value of the maximum on the internal slope of the distribution, on which the density gradients are smaller, cannot be explained only by the increase in fluctuation intensity due to gas compression in the shock because of relatively low fluctuation levels in the free stream. There is obviously an added source of disturbances which is located in the region of the discontinuity of the first derivative of velocity in the shock layer [15]. An estimation of the amplitude of drop oscillations from the peak values on the external slope of the distribution yields 0.2–0.5% of the shock-layer thickness, which has no effect on the distributions of the mean quantities.

Using the measured results of the standard density fluctuations n'_f at the maximum on the internal slope of the mean-density distribution, we calculated the growth rates of disturbances $-\alpha_i$ within the range $x/L = 0.12$–0.33:

$$-\alpha_i = \frac{1}{2}\frac{\partial \ln n'_f}{\partial R}, \qquad R = \sqrt{\mathrm{Re}_{xe}}.$$

For this purpose, n'_f was measured in five cross sections, and a second-order approximation curve was plotted by the least-mean-square method using the measured values. The curve was used to determine the values of the derivative.

Figure 4 shows an experimental curve of $-\alpha_i$ for $R = 210$. The values of $-\alpha_i$ correspond to the growth of disturbances, which for low Reynolds numbers fits the acoustic mode of disturbances [16].

Two-point measurements in the cross section $x/L = 0.33$ on the basis of $\Delta x/L = 0.047$ yielded phase velocities of disturbances c_x/U_e versus the dimensionless frequency F at various points of the shock layer and in the external flow. Figure 5 shows a graph of the phase velocity in the shock layer and in the external flow (curves 1 and 2). The phase-velocity values lie within $c_x/U_e = 0.25$–0.18 and do not depend on the spanwise measurement point. The phase-velocity value supports the assumption of the acoustic nature of the observed disturbances [16], and the proximity of curves 1 and 2 for high free-stream Mach numbers indicates that disturbances are generated on the nozzle walls near the throat.

Figure 6 shows normalized cross-spectra of density fluctuations in the cross section $x/L = 0.33$ for one-point and two-point measurements ($\Delta x/L = 0.047$) in the external flow (points 2 and 4) and in the shock layer (points 1 and 3), respectively. The correlation of density fluctuations drops rapidly with distance between the measurement points for all frequencies: by roughly a factor of 2.5 in the shock layer and by a factor of 1.5

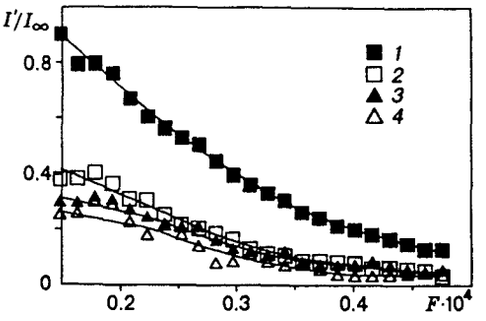

Fig. 6

in the incoming flow. Hence, it follows that the characteristic coherence length l_c in the shock layer is close to $1.7 \cdot 10^{-2}$ m. This is considerably smaller than the flow half-width. Assuming that the spatial characteristics of the coherence scale are isotropic and taking into account the phase-velocity value, in accordance with (2.11), one can speak about legitimacy of density-fluctuation measurements in the given paper over the entire range of frequencies and directions of the wave vector of disturbances. Inequality (2.5) is also satisfied for the values of scale and amplitude of density fluctuations obtained in the paper.

The authors appreciate the assistance of B. A. Sapogov and Yu. A. Safronov in conducting the experiments.

This work was supported by the International Science Foundation (Grants RC9000 and RC9300).

REFERENCES

1. V. R. Gushchin and A. V. Fedorov, "Qualitative features of instability of the wall flow at high supersonic flow speeds," in: *Models of Mechanics of Heterogeneous Media* [in Russian], Inst. of Theor. and Appl. Mech., Sib. Div., Acad. of Sci. of the USSR, Novosibirsk (1989), pp. 93–116.
2. J. A. Smith and J. F. Driscoll, "The electron-beam fluorescence technique for measurements in hypersonic turbulent flows," *J. Fluid Mech.*, **72**, No. 4, 695–719 (1975).
3. J. E. Wallace, "Hypersonic turbulent boundary layer measurements using electron beams," *AIAA J.*, **7**, No. 4, 757–759 (1969).
4. R. L. Bolton and W. D. Harvey, "Use of electron beams for measurements of mean and fluctuating density in hypersonic turbulent shear flow," in: Presentation at the 35th Semi-Annual Meeting of Supersonic Tunnel Association, Dallas, Texas, March 8–9, 1971.
5. V. I. Lysenko, "Stability of a high-speed boundary layer," *Prikl. Mekh. Tekh. Fiz.*, No. 6, 76–78 (1988).
6. M. C. Fisher, D. V. Maddalon, L. M. Weinstein, and R. D. Wagner (Jr.), "Boundary-layer Pitot and hot-wire surveys at M = 20," *AIAA J.*, **9**, No. 5, 826–834 (1971).
7. A. J. Landerman and A. Demetriades, "Mean and fluctuating flow measurements in the hypersonic boundary layer over a cooled wall," *J. Fluid Mech.*, **63**, No. 1, 121–144 (1974).
8. E. P. Muntz, "Measurement of density by analysis of electron beam excited radiation," in: *Methods of Experimental Physics. Fluid Dynamics*, **18** (1981), Part B, pp. 434–355.
9. A. K. Rebrov, G. I. Sukhinin, R. G. Sharafutdinov, and J.-C. Lengrand, "Electron-beam diagnostics in nitrogen. Secondary processes," *Zh. Tekh. Fiz.*, **51**, No. 9, 1832–1840 (1981).
10. I. G. Druker, V. D. Zhak, B. A. Sapogov, and Yu. A. Safronov, "The characteristics of the hypersonic nitrogen wind tunnel T-327 of Inst. of Theor. and Appl. Mechanics, Sib. Div., Acad. of Sci. of the USSR," in: *Problems of Gas Dynamics* [in Russian], Inst. of Theor. and Appl. Mech., Sib. Div., Acad. of Sci. of the USSR, No. 5 (1975).
11. J.-C. Lengrand, J. Allegre, and M. Raffin, "Electron-beam fluorescence technique at relatively high density," Proc. 14th Int. Conf. on Rarefied Gas Dynamics, Tsukuba, 16–20 July, 1984, pp. 828–835.

12. P. J. Harbur and J. N. Lewis, "Preliminary measurement of the hypersonic rarefied flow on a sharp plate using an electron beam probe," in: C. L. Brundin (ed.), *Rarefied Gas Dynamics* (1967), Vol. 2, pp. 1031–1046.
13. J. S. Bendat and A. G. Piersol, *Engineering Applications of Correlation and Spectral Analysis*, John Wiley (1980).
14. G. I. Sukhinin, "On the spatial distribution of parameters of a probing electron beam," in: *Abstract 6th All-Union Conf. on Rarefied Gas Dynamics*, Inst. of Thermal Phys., Sib. Div., Acad. of Sci. of the USSR, Novosibirsk (1979), pp. 79–81.
15. A. A. Maslov, S. G. Mironov, and Yu. A. Safronov, "Velocity measurements on a flat plate in the hypersonic flow by electron-beam fluorescence," in: *Proc. Int. Conf. on the Methods of Aerophysical Research*, ITAM SB RAS, Novosibirsk (1994), Part 2, pp. 178–182.
16. S. A. Gaponov and A. A. Maslov, *Development of Disturbances in Compressible Flows* [in Russian], Nauka, Novosibirsk (1980).